

BASIC RESEARCH PAPER

## Acetylation targets HSD17B4 for degradation via the CMA pathway in response to estrone

Ye Zhang<sup>a,#</sup>, Ying-Ying Xu<sup>a,#</sup>, Chuan-Bo Yao<sup>a</sup>, Jin-Tao Li<sup>a</sup>, Xiang-Ning Zhao<sup>a</sup>, Hong-Bin Yang<sup>a</sup>, Min Zhang<sup>a</sup>, Miao Yin<sup>a</sup>, Jing Chen<sup>b</sup>, and Qun-Ying Lei<sup>a</sup>

<sup>a</sup>Key Laboratory of Metabolism and Molecular Medicine, Ministry of Education, and Department of Biochemistry and Molecular Biology, School of Basic Medical Sciences, and Cancer Metabolism Laboratory, Institutes of Biomedical Sciences, and State Key Laboratory of Medical Neurobiology, Fudan University, Shanghai, China; <sup>b</sup>Department of Hematology and Medical Oncology, Winship Cancer Institute of Emory, Emory University School of Medicine, Atlanta, GA, USA

### ABSTRACT

Dysregulation of hormone metabolism is implicated in human breast cancer.  $17\beta$ -hydroxysteroid dehydrogenase type 4 (*HSD17B4*) catalyzes the conversion of estradiol (E2) to estrone (E1), and is associated with the pathogenesis and development of various cancers. Here we show that E1 upregulates *HSD17B4* acetylation at lysine 669 (K669) and thereby promotes *HSD17B4* degradation via chaperone-mediated autophagy (CMA), while a single mutation at K669 reverses the degradation and confers migratory and invasive properties to MCF7 cells upon E1 treatment. CREBBP and SIRT3 dynamically control K669 acetylation level of *HSD17B4* in response to E1. More importantly, K669 acetylation is inversely correlated with *HSD17B4* in human breast cancer tissues. Our study reveals a crosstalk between acetylation and CMA degradation in *HSD17B4* regulation, and a critical role of the regulation in the malignant progression of breast cancer.

### ARTICLE HISTORY

Received 27 May 2016  
Revised 17 November 2016  
Accepted 30 November 2016






### KEYWORDS

acetylation; cancer; chaperone-mediated autophagy; estrone; *HSD17B4*

### Introduction


Breast cancer is a leading cause of female death worldwide.<sup>1</sup> It has been shown that growth of normal human breast tissue is estrogen dependent, and most breast cancers are estrogen receptor-positive.<sup>2</sup> Normal growth and function of the breast are under moderate hormone control, while excessive hormonal stimulation may induce tumor formation.<sup>3</sup> Estrogen influences multiple biological responses in cells, and therefore affects the growth, motility and invasiveness of cancer cells.<sup>4–6</sup> The main estrogens circulating in the human body are E2 and E1. E2 is the most potent and active form of estrogen, whereas E1 is the less active form of estrogen. HSD17B1 ( $17\beta$ -hydroxysteroid dehydrogenase1) is the most active enzyme to produce E2<sup>7–10</sup> and significantly overexpressed in breast cancer, which contributes to the stimulation and development of breast cancer.<sup>11,12</sup> HSD17B2, which converts E2 to E1, is dominant in normal breast.<sup>13</sup> Studies have shown that increased HSD17B1 expression or ratio of HSD17B1 and HSD17B2 expression is associated with poor clinical outcome of estrogen-dependent breast cancer patients.<sup>12,14</sup> Besides HSD17B1, HSD17B7 has been identified as a key enzyme for the viability of breast cancer due to the dual functions on activation and reduction of estrogen and androgen.<sup>15</sup>

HSD17B4, catalyzing the conversion of estradiol (E2) to estrone (E1),<sup>16,17</sup> is strongly conserved in sequence and functionality.<sup>18</sup> It is also known as D-3-hydroxylacyl-CoA dehydrogenase, D-specific bifunctional protein (DBP), multifunctional protein 2 (MFP-2) or peroxisomal multifunctional enzyme type2 (MFE-2), and displays multifunctional properties, including bile acid biosynthesis, fatty acid  $\beta$ -oxidation, sterol transport and sex steroid metabolism.<sup>16,19,20</sup> Recent evidence has shown that *HSD17B4* is implicated in cancer. It is reported that *HSD17B4* is overexpressed in prostate cancer, compared with matched-benign epithelium.<sup>21</sup> Therefore *HSD17B4* is regarded as an independent biomarker of poor patient outcome in prostate cancer.<sup>21</sup> *HSD17B4* is ubiquitously expressed in liver with highest levels, and implicates in the pathogenesis and development of human hepatocellular carcinoma (HCC) via inactivating E2.<sup>22</sup> Previous studies also indicate that the loss of estrogen inactivation may be an important mechanism in the pathogenesis of colonic cancer, suggesting a potential role of *HSD17B4* in colonic cancer.<sup>23,24</sup> Similarly, *HSD17B4* is overexpressed in ovarian surface epithelium (hOSE) cells and might prevent an excessive accumulation of E2 in the human ovary by inactivating estrogen,<sup>25</sup> which thus provided therapeutic targets for ovary cancer prevention and treatment.<sup>26</sup> NF $\kappa$ B1 can upregulate

**CONTACT** Miao Yin  [miaoyin@fudan.edu.cn](mailto:miaoyin@fudan.edu.cn)  Key Laboratory of Metabolism and Molecular Medicine, Ministry of Education, and Department of Biochemistry and Molecular Biology, School of Basic Medical Sciences, and Cancer Metabolism Laboratory, Institutes of Biomedical Sciences, and State Key Laboratory of Medical Neurobiology, Fudan University, Shanghai, China; Jing Chen  [jchen@emory.edu](mailto:jchen@emory.edu)  Department of Hematology and Medical Oncology, Winship Cancer Institute of Emory, Emory University School of Medicine, Atlanta, GA, USA; Qun-Ying Lei  [qlei@fudan.edu.cn](mailto:qlei@fudan.edu.cn)

Color versions of one or more of the figures in the article can be found online at [www.tandfonline.com/kaup](http://www.tandfonline.com/kaup).

<sup>#</sup>These authors contributed equally to this work.

 Supplemental data for this article can be accessed on the publisher's website.

*HSD17B4* expression in HCC, which is due to the fact that the *HSD17B4* gene contains NF $\kappa$ B1-binding sites. TNF upregulates *HSD17B4* expression via NF $\kappa$ B1 and then promotes the acquisition of a transformed phenotype during hepatocarcinogenesis.<sup>22,27</sup> Moreover, it has been reported that *HSD17B4* expression may be regulated by promoter methylation and mRNA stabilization.<sup>28-30</sup> Methylation of the *HSD17B4* promoter is also found in ERBB2/HER-2/neu-positive breast cancers.<sup>29</sup> Here we propose the posttranslational regulation of *HSD17B4* expression. We presently demonstrate that *HSD17B4* protein is acetylated at lysine residue 669 and this acetylation modification promotes *HSD17B4* lysosome-dependent degradation via chaperone-mediated autophagy (CMA). Interestingly, K669 acetylation of *HSD17B4* was modulated by extracellular E1. Our study reveals an acetylation regulation of *HSD17B4* and its potential function in tumor development.

## Results

### *HSD17B4* is acetylated at lysine 669 to promote its degradation via autophagy

Several mass spectrometry (MS) analyses suggested that *HSD17B4* was potentially an acetylated protein (Fig. S1A). To confirm the acetylation modification, we transfected FLAG-*HSD17B4* into HEK293T cells and detected the acetylation level of ectopically expressed *HSD17B4* using a pan acetyl-lysine antibody. Results showed that trichostatin A (TSA, an inhibitor of histone deacetylase HDAC family I, II and IV) and nicotinamide (NAM, an inhibitor of the SIRT family deacetylase) treatment significantly increased the acetylation level of FLAG-*HSD17B4* (Fig. 1A), indicating that *HSD17B4* is indeed acetylated. Since various lysine (K) residues have been reported as potential acetylation sites, we then mutated each of 5 lysine residues individually to arginine (R), and examined their acetylation. Mutation of K669, but not other lysine residues, resulted in a significant reduction in acetylation level of ectopically expressed *HSD17B4* (Fig. 1B and C). Notably, TSA and NAM treatment increased the acetylation level of wild-type *HSD17B4*, but not the K669R mutant (Fig. 1C), implying K669 is the main acetylation site of *HSD17B4*. Acetylation of K669 in peptide WTIDLK(ac)SGSGK was hit twice with a high score and matched the human *HSD17B4* sequence with acetylation at K669 by 2 different proteomic studies.<sup>31,32</sup> To confirm K669 acetylation of *HSD17B4*, we generated a K669 site-specific antibody (designated as 'K669Ac antibody' henceforth) which specifically targeted the acetylated K669 residue in *HSD17B4*. First we performed dot blotting assays to characterize the specificity of the K669Ac antibody and found that this antibody preferentially detected the K669-acetylated, but not the unmodified peptide (Fig. S1B). The peptide blocking experiment showed that the K669-acetylated peptide absorbed the K669Ac antibody, and therefore decreased K669Ac signal (Fig. S1C). These results indicated a high specificity of this antibody to *HSD17B4* K669 acetylation. With the help of this site-specific antibody, we detected enhanced K669 acetylation signals in HEK293T, MCF7 and MDA-MB-231 cells upon NAM, but not TSA treatment (Fig. 1D), further supporting that K669 is the major acetylation site of *HSD17B4* under this condition. Interesting, under the

same conditions, we detected significantly decreased levels of endogenous *HSD17B4* protein in NAM-treated HEK293T, MCF7 and MDA-MB-231 cells (Fig. 1D), suggesting a role of acetylation in regulating *HSD17B4* expression.

Previous studies report that lysine acetylation modulates the degradation of multiple protein.<sup>33-35</sup> To elucidate the mechanism that K669 acetylation modulates in the regulation of *HSD17B4* expression, we first examined *HSD17B4* mRNA and found that NAM did not downregulate *HSD17B4* protein at the transcriptional level (Fig. S1D). Next, chloroquine (CLQ, an inhibitor of lysosomal proteases) and bafilomycin A<sub>1</sub> (BAF), (an inhibitor of the vacuolar-type H<sup>+</sup>-translocating ATPase and frequently used to block late-phase autophagy) (Fig. 1E and S1E), but not MG132 (a proteasome inhibitor) treatment (Fig. S1F), rescued the decrease of *HSD17B4* protein induced by NAM. These results indicate that the NAM-induced decrease of *HSD17B4* is due to the lysosome system or autophagy, but not proteasome-dependent degradation. Moreover, we found that treatment with leupeptin (another inhibitor of lysosomal proteases) led to an accumulation of *HSD17B4* protein and a significant increase in K669 acetylation (Fig. 1F), implying the involvement of autophagy in K669 acetylation-induced *HSD17B4* degradation.

### *HSD17B4* degradation induced by acetylation requires CMA

The lysosome system or autophagy can participate in protein degradation. There are 3 autophagy mechanisms reported, macroautophagy, microautophagy, and chaperone-mediated autophagy (CMA). CMA is thought to selectively degrade many long-half-life proteins.<sup>36</sup> In order to verify which mechanism is responsible for *HSD17B4* degradation, we treated HEK293T, MCF7 and MDA-MB-231 cells with the lysosomal inhibitor NH<sub>4</sub>Cl, the ubiquitin proteasome inhibitor MG132 and the macroautophagy inhibitors 3-methyladenine (3-MA) and wortmannin respectively, and determined the levels of total *HSD17B4* protein by western blotting. Results showed that NH<sub>4</sub>Cl, but not MG132, 3-MA or wortmannin, induced the accumulation of *HSD17B4* protein (Fig. 2A and S2A), indicating that the degradation of *HSD17B4* is independent of the proteasome and macroautophagy pathways. To validate the relationship between K669 acetylation and *HSD17B4* degradation, a serum-deprivation experiment was conducted and the results showed increased K669 acetylation levels and decreased *HSD17B4* protein levels, which corresponded with the extended time of serum deprivation (Fig. 2B). Based on the findings that prolonged serum deprivation can activate CMA,<sup>37,38</sup> and our data that 3-MA or wortmannin treatment did not change *HSD17B4* acetylation at K669 and its protein levels (Fig. 2B), these results suggest that K669 acetylation promotes *HSD17B4* degradation through the CMA pathway.

During CMA, the chaperone heat shock protein HSPA8/HSC70 carries target proteins to the lysosomal receptor LAMP2A, which then translocates the target proteins into the lysosome for degradation.<sup>37</sup> To provide more evidence for CMA, we knocked down HSPA8 in HEK293T cells and found an increased protein level of *HSD17B4* (Fig. 2C). To explore the effect of K669 acetylation on *HSD17B4* degradation

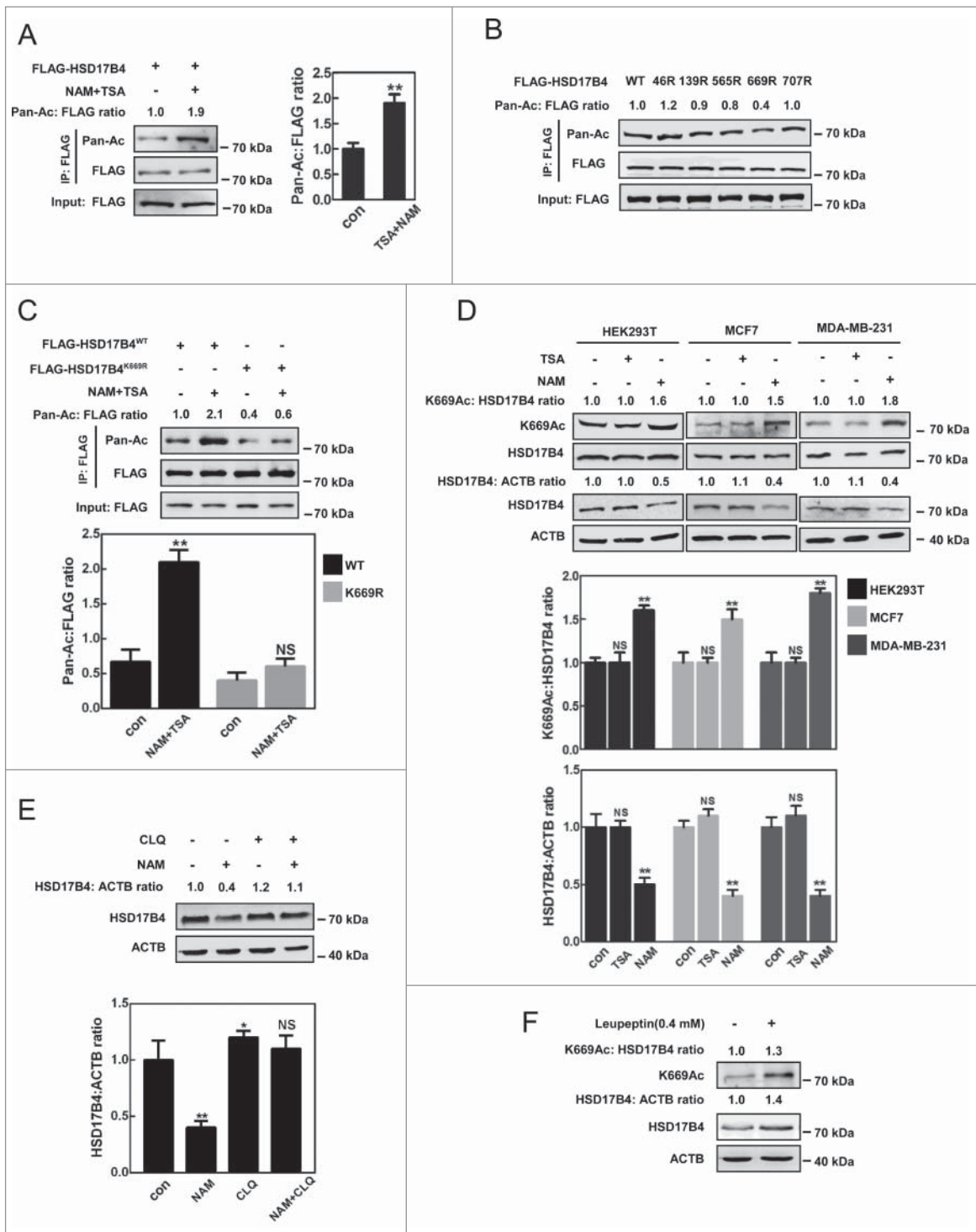


**Figure 1.** HSD17B4 is acetylated at lysine 669 to promote its degradation via autophagy. (A) Exogenous HSD17B4 is acetylated. FLAG-HSD17B4 was transfected into HEK293T cells, followed by TSA (10  $\mu$ M) and NAM (5 mM) treatment. FLAG-HSD17B4 acetylation was detected with anti-acetyl lysine (Pan-Ac) antibody by western blotting (left panel). Relative HSD17B4 acetylation over FLAG-HSD17B4 level was quantified (right panel). \*\*denotes  $P < 0.01$ , Error bars represent  $\pm$  SD for triplicate experiments. (B) Analysis of acetylation of individual HSD17B4 mutants. The indicated plasmids were transfected into HEK293T cells and protein lysates were immunoprecipitated for acetylation analysis. (C) TSA and NAM treatment increases acetylation level of wild-type HSD17B4 but not mutants. Ectopically expressed wild-type HSD17B4 and the K669R mutant were transfected into HEK293T cells respectively, followed by TSA and NAM treatment. HSD17B4 acetylation was analyzed by western blotting (upper panel). The relative HSD17B4 acetylation over the FLAG-HSD17B4 level was quantified (lower panel). \*\*denotes  $P < 0.01$ , NS denotes no significance. Error bars represent  $\pm$  SD for triplicate experiments. (D) NAM but not TSA increases HSD17B4 acetylation level at K669, while decreases the endogenous HSD17B4 protein level. HEK293T, MCF7 or MDA-MB-231 cells were treated with NAM or TSA. HSD17B4 protein was determined by western blotting and normalized against ACTB, K669 acetylation was detected with K669Ac antibody and normalized against HSD17B4 protein. The relative HSD17B4 K669 acetylation compared with total protein level and the relative HSD17B4 protein compared with the ACTB level were quantified (lower panel). \*denotes  $P < 0.05$ ; NS, no significance. Error bars represent  $\pm$  SD for triplicate experiments. (E) Chloroquine (CLQ) restores HSD17B4 protein reduced by NAM treatment. HEK293T cells were treated as indicated and HSD17B4 protein was determined by western blotting (upper panel). The relative HSD17B4 protein compared with the ACTB level was quantified (lower panel). \*\*denotes  $P < 0.01$ , \*denotes  $P < 0.05$ . Error bars represent  $\pm$  SD for triplicate experiments. (F) Leupeptin accumulates K669-acetylated and total HSD17B4 protein. HEK293T cells were treated with leupeptin for 48 h. The levels of total and acetylated HSD17B4 were determined by western blotting. HSD17B4 protein levels were normalized against ACTB. K669 acetylation levels were normalized against HSD17B4 protein.

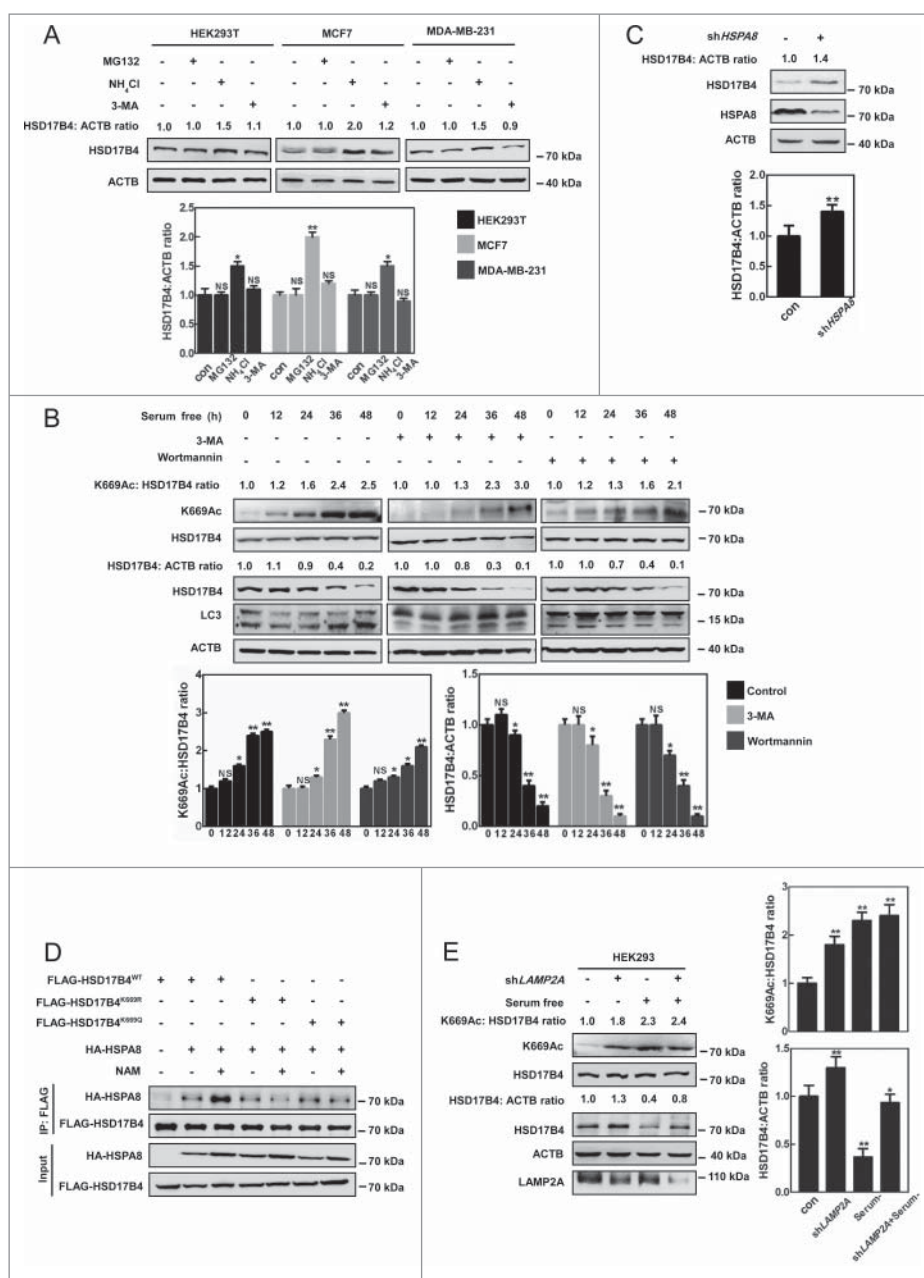


**Figure 2.** HSD17B4 degradation induced by acetylation requires CMA. (A) Lysosome inhibitor NH<sub>4</sub>Cl accumulates HSD17B4 protein, while the ubiquitin proteasome inhibitor MG132 or macroautophagy inhibitor 3-MA does not. HEK293T, MCF7 or MDA-MB-231 cells were treated as indicated. The levels of total HSD17B4 protein were determined by western blotting (upper panel). Relative HSD17B4 protein compared with ACTB levels were quantified (lower panel). \*\*denotes  $P < 0.01$ ; NS, no significance. Error bars represent  $\pm$  SD for triplicate experiments. (B) Serum deprivation decreases HSD17B4 protein while it increases its acetylation level. HEK293T cells were cultured upon serum deprivation for different lengths of time as indicated. HSD17B4 levels were normalized against ACTB, K669 acetylation was normalized against HSD17B4 protein, analyzed by western blotting (upper panel). The relative HSD17B4 K669 acetylation compared with total protein level and the relative HSD17B4 protein compared with the ACTB level were quantified (lower panel). \*\*denotes  $P < 0.01$ , \*denotes  $P < 0.05$ ; NS, no significance. Error bars represent  $\pm$  SD for triplicate experiments. (C) HSPA8 knockdown accumulates HSD17B4 protein. HSPA8 was transiently knocked down in HEK293T cells by shRNA. HSD17B4 protein and the knockdown efficiency were determined by western blotting (upper panel). Relative HSD17B4 protein levels compared with ACTB were quantified (lower panel). \*\*denotes  $P < 0.01$ . Error bars represent  $\pm$  SD for triplicate experiments. (D) NAM promotes wild-type HSD17B4 binding with HSPA8 but not K669 mutants. Ectopically expressed wild-type HSD17B4, as well as the K669R or K669Q mutant were cotransfected with a plasmid expressing HSPA8 into HEK293T cells followed by NAM treatment; the binding between HSD17B4 and HSPA8 was analyzed by western blotting. (E) LAMP2A knockdown restores the decreased HSD17B4 protein induced by serum deprivation. HEK293 cells stably expressing LAMP2A shRNA were cultured with or without serum. The levels of K669 acetylation, HSD17B4 and LAMP2A proteins were determined by western blotting (left panel). The relative HSD17B4 K669 acetylation compared with its total protein level and the relative HSD17B4 protein compared with the ACTB level were quantified (right panel). \* denotes  $P < 0.05$ , \*\*denotes  $P < 0.01$ . Error bars represent  $\pm$  SD for triplicate experiments.

through CMA, we performed coimmunoprecipitation and found that NAM treatment significantly enhanced the binding between ectopically expressed wild-type HSD17B4 and HSPA8, while the K669R or K669Q mutant of HSD17B4 did not display a stronger interaction with HSPA8 after NAM treatment

(Fig. 2D and S2B). Consistently, we knocked down LAMP2A in HEK293 cells and observed an accumulation of HSD17B4 protein upon either normal condition or serum deprivation (Fig. 2E and S2C). These data support that CMA is responsible for acetylation-induced degradation of HSD17B4.

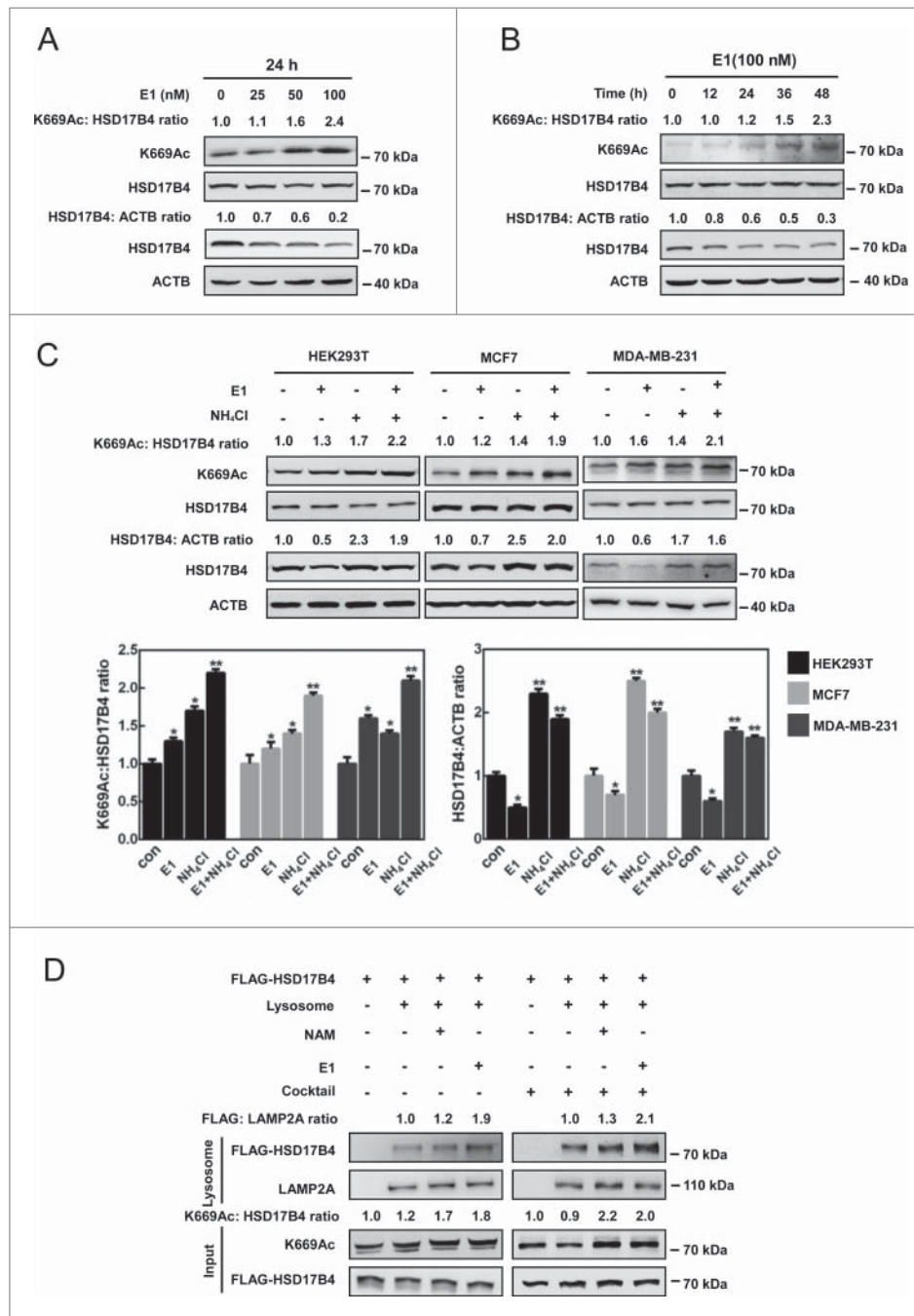


**Figure 3.** E1 increases HSD17B4 acetylation at K669 to promote its degradation via CMA. (A and B) E1 treatment increases HSD17B4 K669 acetylation level but decreases endogenous HSD17B4 protein level. MCF7 cells were either untreated or treated with E1 for different concentration (A) or different lengths of time (B), as indicated. The steady-state levels of HSD17B4 protein were determined by western blotting and normalized against ACTB, and K669 acetylation was normalized against HSD17B4 protein. (C) E1 increases K669 acetylation level and promotes HSD17B4 degradation through a lysosomal pathway. HEK293T, MCF7 or MDA-MB-231 cells were treated with E1 and NH<sub>4</sub>Cl as indicated, followed by being lysed and subjected to western blotting (upper panel). The relative HSD17B4 K669 acetylation compared with total protein level and the relative HSD17B4 protein compared with the ACTB level were quantified (lower panel). \*\*denotes  $P < 0.01$ , \*denotes  $P < 0.05$ . Error bars represent  $\pm$  SD for triplicate experiments. (D) K669 acetylation promotes lysosomal uptake of HSD17B4. FLAG-tagged HSD17B4 was immunopurified from HEK293T cells treated with or without NAM and E1, and incubated with the lysosomes isolated from rat liver. Lysosomes were re-isolated and the associated HSD17B4 (either inside or binding to the surface) was determined by western blotting. The presence of protease inhibitors (cocktail) should block lysosomal degradation; thus, such conditions should measure both HSD17B4 binding to lysosomes and uptake, whereas in the absence of cocktail only measures HSD17B4 binding to lysosomes.

### E1 increases HSD17B4 acetylation at K669 to promote its degradation via CMA

E1 is one of the products of *HSD17B4*, which plays an essential role in cancer development and progression.<sup>25</sup> To determine whether E1 dynamically regulates *HSD17B4* protein level in breast cancer, we cultured MCF7 cells under hormone-deprived

conditions for 24 h, followed by treating the cells with E1 at different concentrations for another 24 h, and found that 100 nM E1 dramatically increased K669 acetylation while it decreased the protein level of *HSD17B4* (Fig. 3A). Further results indicated that E1 increased K669 acetylation and promoted *HSD17B4* degradation in a time-dependent manner (Fig. 3B). Moreover, the unchanged mRNA level of *HSD17B4* upon E1 treatment

proves that E1 regulates *HSD17B4* expression at a post-transcriptional level (Fig. S3). We then explored the effect of the inhibitor of lysosomal proteases and found that  $\text{NH}_4\text{Cl}$  restored the *HSD17B4* protein level reduced by E1 treatment in HEK293T, MCF7 and MDA-MB-231 cells (Fig. 3C). In agreement with the protein levels, K669 acetylation of *HSD17B4* was enhanced by E1 treatment (Fig. 3C), suggesting a model in which E1 increases *HSD17B4* acetylation and thereby promotes its lysosomal degradation. To validate the involvement of lysosome in *HSD17B4* degradation, we incubated immunopurified *HSD17B4* with isolated lysosomes in vitro and found that *HSD17B4* binds to lysosomes (Fig. 3D). In the presence of lysosomal protease inhibitors, this assay showed the total *HSD17B4*, which was bound to and taken up by the lysosomes. Notably, the *HSD17B4* isolated from NAM- or E1-treated cells showed more lysosomal binding and uptake than *HSD17B4* isolated from untreated cells (Fig. 3D). These results demonstrate that E1 enhances K669 acetylation and promotes the degradation of *HSD17B4* through the lysosome system.

To further investigate the mechanisms of *HSD17B4* degradation induced by E1, we knocked down *LAMP2A* in MCF7 and MDA-MB-231 cells to disrupt CMA, and found a significant accumulation of *HSD17B4* protein in the presence of E1, associating with a further increase of K669 acetylation (Fig. 4A). Moreover, E1 exclusively increased the interaction between HSPA8 and wild-type *HSD17B4*, but not the K669R or K669Q mutant (Fig. 4B). Consistently, the enhanced binding between endogenous *HSD17B4* and HSPA8 was also observed upon E1 treatment (Fig. 4C). Similarly, E1 also increased the interaction between endogenous *HSD17B4* and *LAMP2A* (Fig. 4C).

Confocal microscopy data showed that K669-acetylated *HSD17B4* accumulated in lysosomes in the presence of  $\text{NH}_4\text{Cl}$ , indicating that acetylated *HSD17B4* is a potential substrate of CMA (Fig. 4D and E). We next determined whether E1 contributed to CMA activation in the total lysosomal pool in MCF7 cells. Since the lysosome marker *LAMP2A* and HSPA8 increase with the enhanced CMA activity,<sup>39-42</sup> we investigated the colocalization of lysosomal *LAMP2A* and HSPA8 by immunofluorescence in cultured cells maintained in the presence or absence of E1, and found that the number of positive colocalized protein was higher in E1-treated cells, which revealed an increased CMA activity (Fig. S4A and S4B). Costaining of *HSD17B4* and lysosomal marker also indicates that E1 promotes colocalization of *HSD17B4* and *LAMP2A* (Fig. 4F and G), consistent with a promoting role of E1 in *HSD17B4* degradation through CMA.

Taken together, these data indicate that E1-induced K669 acetylation promotes *HSD17B4* degradation through CMA.

### CREBBP acetylates HSD17B4 at K669

To identify the acetyl-transferase responsible for *HSD17B4* K669 acetylation, we transfected DNA encoding 4 acetyltransferases, CREBBP (CREB binding protein), EP300 (E1A binding protein p300), KAT2A (lysine acetyltransferase 2A), and KAT2B, (lysine acetyl-transferase 2B), individually into HEK293T cells, and found that CREBBP overexpression distinctively increased K669 acetylation level, as well as inversely decreased *HSD17B4* protein (Fig. 5A). This downregulation of *HSD17B4* protein could be

blocked by CLQ or BAF treatment (Fig. 5B and S5), indicating the positive role of CREBBP in K669 acetylation-induced degradation of *HSD17B4*. Further experiments showed that CREBBP increased the levels of K669 acetylation in a dose-dependent manner (Fig. 5C). Consistently with our hypothesis, CREBBP knockdown dramatically decreased K669 acetylation of *HSD17B4* and inversely increased its protein level (Fig. 5D). Furthermore, CREBBP knockdown blocked the E1-induced decrease of *HSD17B4* protein (Fig. 5E). In MCF7 cells, the binding between endogenous *HSD17B4* and CREBBP was detected and indeed enhanced by E1 treatment (Fig. 5F). Collectively, our results demonstrate that CREBBP is mainly the acetyltransferase responsible for *HSD17B4* acetylation at K669 and plays an important role in *HSD17B4* degradation.

### SIRT3 deacetylates HSD17B4 at K669

According to the results that NAM, an inhibitor of SIRT deacetylases, increased K669 acetylation of *HSD17B4* (Fig. 1D), we supposed that SIRT family members might participate in *HSD17B4* deacetylation. Thereafter we overexpressed SIRT1-7 individually, and found that SIRT3, but not others, decreased the K669 acetylation level of endogenous *HSD17B4* (Fig. 6A). Consistently, HA-tagged SIRT3 significantly decreased K669 acetylation levels of exogenous and endogenous *HSD17B4* in HEK293T cells (Fig. 6B and 6C), whereas the inactive H248Y mutant of SIRT3 had no effect on *HSD17B4* acetylation (Fig. 6C). These data demonstrate that SIRT3 is responsible for K669 acetylation of *HSD17B4*.

Based on the conclusion that K669 acetylation of *HSD17B4* promotes its degradation, we investigated whether SIRT3 affected the protein level of *HSD17B4*. The results indicated that SIRT3 overexpression increased *HSD17B4* protein (Fig. 6D). Consistently, SIRT3 knockdown reduced *HSD17B4* protein (Fig. 6E), which was blocked by  $\text{NH}_4\text{Cl}$  treatment (Fig. 6F). Moreover, SIRT3 knockdown dramatically enhanced K669 acetylation (Fig. 6E) and  $\text{NH}_4\text{Cl}$  treatment further accumulated acetylated *HSD17B4* protein (Fig. 6F). These results suggest a resistant effect of SIRT3 in *HSD17B4* lysosomal degradation. Confocal microscopy data indicated the interaction between SIRT3 and *HSD17B4* (Fig. S6A). More evidence was obtained when we found the binding between endogenous *HSD17B4* and SIRT3, which was not affected by CLQ or  $\text{NH}_4\text{Cl}$  (Fig. S6B), was attenuated by E1 treatment (Fig. 6G). Collectively, SIRT3 deacetylates *HSD17B4* at K669 and stabilizes *HSD17B4*.

### K669 mutants increase cell migration and invasion

To investigate whether *HSD17B4* is essential for cancer cells, we knocked down endogenous *HSD17B4* in MCF7 breast cancer cells by shRNA at the 3' UTR and re-expressed the wild-type, as well as the K669R and K669Q mutants of *HSD17B4* to a level similar to endogenous *HSD17B4* (Fig. 7A). Consistent with our previous results, E1 caused a notable decrease of wild-type *HSD17B4* in the stable cells, but had no effect on the K669R and K669Q mutants (Fig. 7B). Interestingly, we explored the stable cells cultured under normal or E1 condition and found an increase of

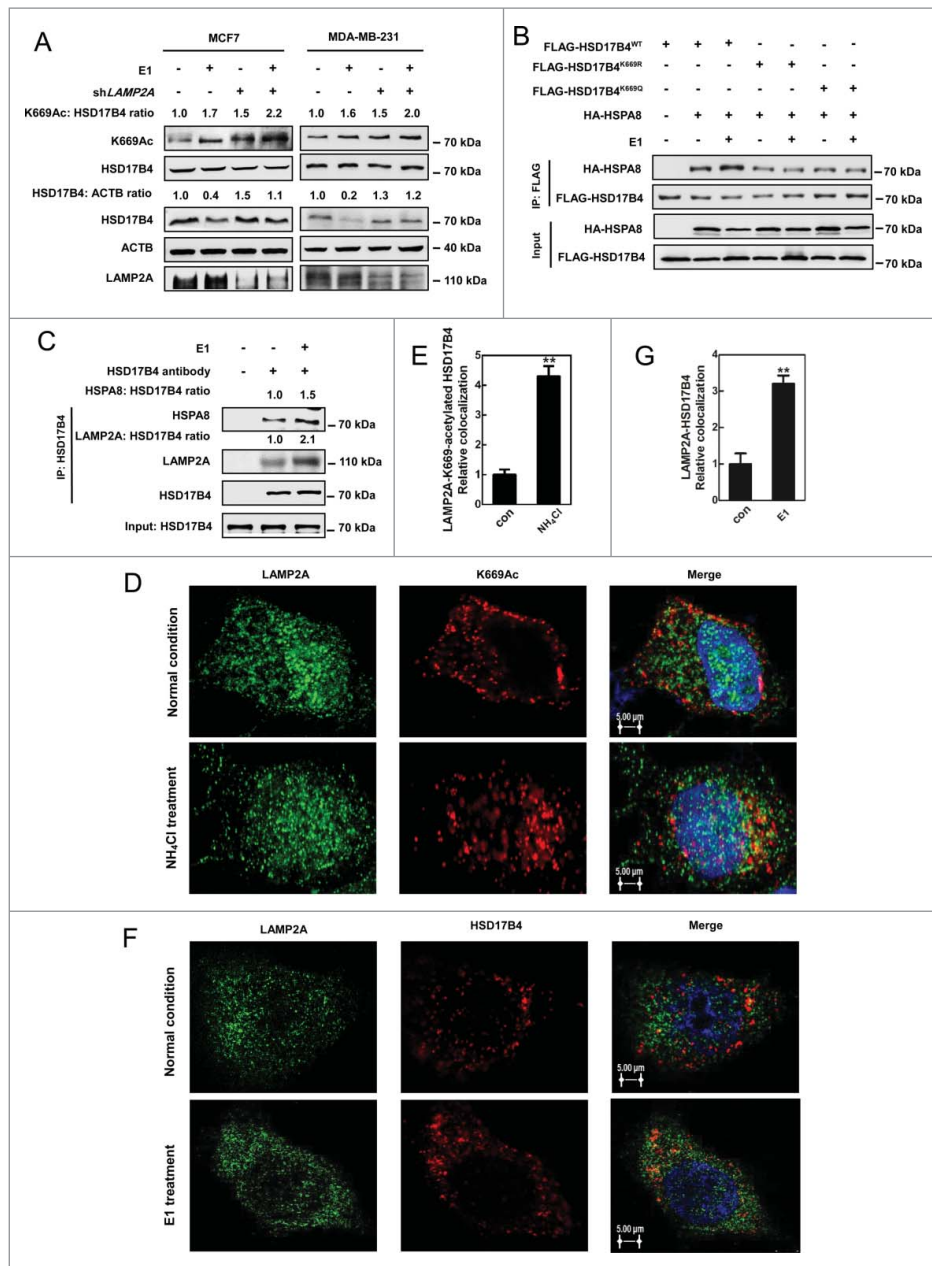


**Figure 4.** HSD17B4 is a substrate of CMA. (A) *LAMP2A* knockdown restores the decreased HSD17B4 protein induced by E1 treatment. MCF7 or MDA-MB-231 cells transiently expressing *LAMP2A* shRNA were cultured with or without E1. HSD17B4 protein was determined by western blotting and normalized against ACTB, K669 acetylation was detected with K669Ac antibody and normalized against HSD17B4 protein. (B) E1 promotes HSPA8 binding with wild-type HSD17B4 but not the K669R or K669Q mutant. Ectopically expressed wild-type HSD17B4, as well as the K669R or K669Q mutant were cotransfected with a plasmid expressing HSPA8 into HEK293T cells followed by E1 treatment for 24 h, the binding between HSD17B4 and HSPA8 was analyzed by coIP and western blotting. (C) E1 promotes endogenous HSD17B4 binding with HSPA8 or LAMP2A in MCF7 cells. MCF7 cells were cultured with or without E1 for 24 h before harvest. The interaction between endogenous HSD17B4 and HSPA8 or LAMP2A was determined by coimmunoprecipitation and western blotting. (D and E) NH<sub>4</sub>Cl accumulates K669 acetyl-HSD17B4 in lysosomes. MCF7 cells were cultured with or without NH<sub>4</sub>Cl for 24 h as indicated, then paraformaldehyde fixed, blocked, and processed for double immunofluorescence with antibodies against LAMP2A (green) and K669Ac (red). Merged images of both channels are shown on the right. Bar: 5  $\mu$ m (D). Relative LAMP2A colocalization with K669 acetyl-HSD17B4 was calculated using ImageJ software; the ratio was quantified. Mean values were calculated from the individual distributions in 10 cells per condition (E). (F and G) E1 enhances the interaction between HSD17B4 and LAMP2A. MCF7 cells were cultured with or without E1 for 24 h as indicated, then paraformaldehyde fixed, blocked, and processed for double immunofluorescence with antibodies against LAMP2A (green) and HSD17B4 (red). Merged images of both channels are shown on the right. Bar: 5  $\mu$ m (F). Relative LAMP2A colocalization with HSD17B4 was calculated using ImageJ software; the ratio was quantified. Mean values were calculated from the individual distributions in 10 cells per condition (G).

CDH1/E-Cadherin (cadherin 1) but a decrease of CDH2/N-Cadherin (cadherin 2) and VIM (vimentin) in MCF7 cells expressing wild-type *HSD17B4* (Fig. 7B). Loss of CDH1 and acquirement of CDH2 as well as VIM constitute epithelial-mesenchymal transition (EMT) biomarker signals. Together with the result that E1 destabilized wild-type *HSD17B4*, this datum suggests that E1-induced *HSD17B4* acetylation at

K669 decreases its protein level and then inhibits the EMT tendency of cancer cells.

EMT is a conserved and reversible biological process characterized by the transition of cells from epithelial phenotype to mesenchymal properties. During EMT, cells lose their cell polarity and cell-cell adhesion, and simultaneously gain a mesenchymal morphology promoting migration and

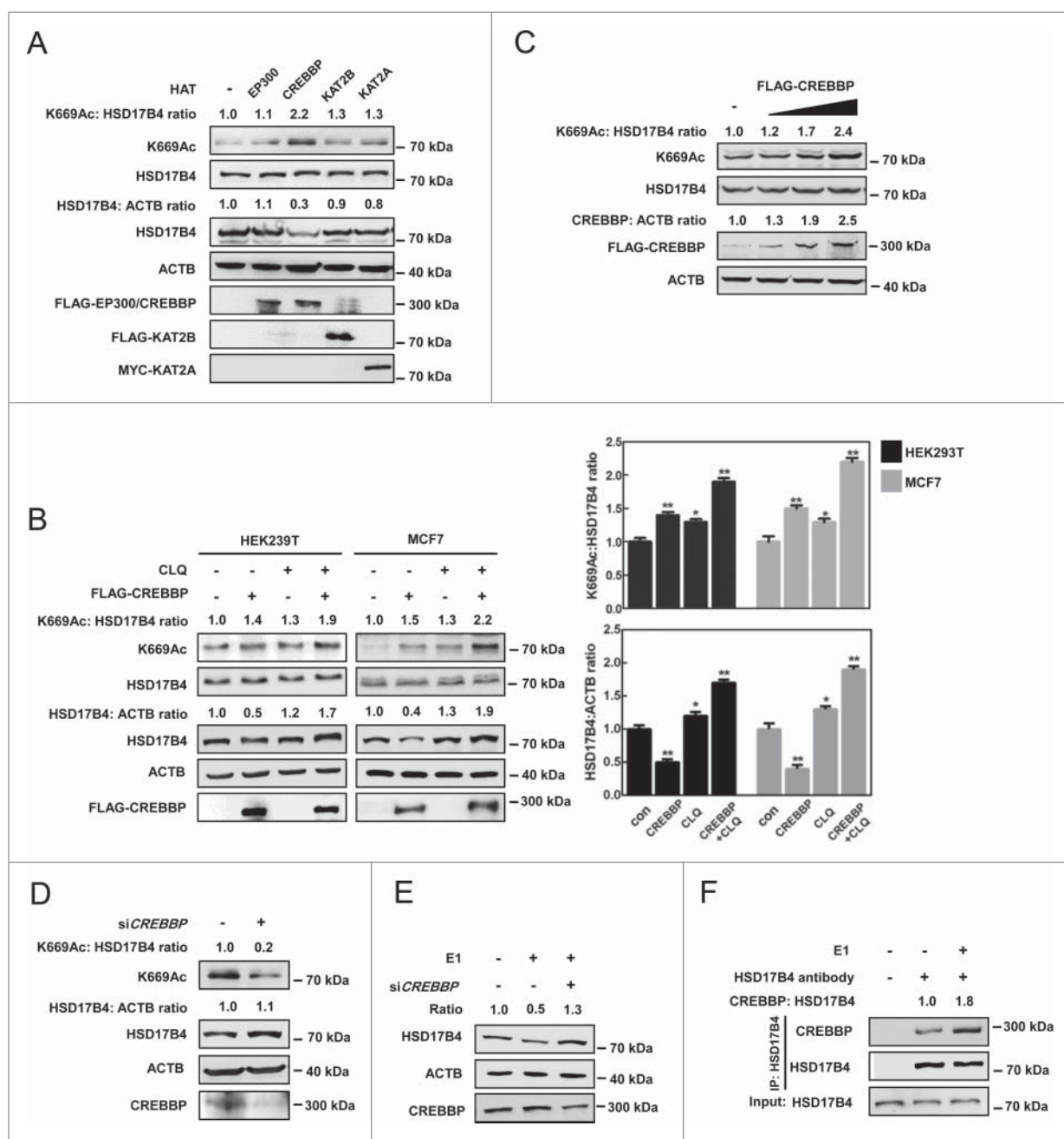


**Figure 5.** CREBBP acetylates HSD17B4 at K669. (A) Overexpression of CREBBP, not other HATs, decreases the protein level but increases the K669 acetylation level of endogenous HSD17B4. HEK293T cells were transfected as indicated. Cell lysates were subjected to western blotting. HSD17B4 levels were normalized against ACTB. K669 acetylation was normalized against HSD17B4 protein. (B) CLQ blocks the reduction of HSD17B4 protein induced by CREBBP overexpression. FLAG-CREBBP was transfected into MCF7 cells and HEK293T cells with or without CLQ treatment and cell lysates were measured by western blotting (left panel). The relative HSD17B4 K669 acetylation compared with total protein level and the relative HSD17B4 protein compared with the ACTB level were quantified (right panel). \*denotes  $P < 0.05$ , \*\*denotes  $P < 0.01$ . Error bars represent  $\pm$  SD for triplicate experiments. (C) CREBBP increases K669 acetylation levels of HSD17B4. FLAG-CREBBP was transfected in ascending doses into HEK293T cells and cell lysates were measured by western blotting. (D) CREBBP knockdown decreases HSD17B4 K669 acetylation while it causes accumulation of the total protein. HEK293T cells were transfected with siCREBBP or control. HSD17B4 acetylation and protein levels were determined by western blotting. (E) CREBBP knockdown blocks E1-induced degradation of HSD17B4. MCF7 cells were transfected with siCREBBP or control and cultured in the presence of E1. Protein levels of endogenous HSD17B4 were determined by western blotting and normalized against ACTB. (F) E1 promotes endogenous HSD17B4 binding with CREBBP in MCF7 cells. MCF7 cells were cultured with or without E1 for 24 h before harvest. The interaction between endogenous HSD17B4 and CREBBP was determined by coIP and western blotting.

invasion. EMT features benefit metastasis and malignant progression of various neoplasia.<sup>43,44</sup> To further explore the effect of HSD17B4 acetylation on cancer cells, we first performed wound-healing assays. Results showed that HSD17B4 knockdown inhibited the migration of MCF7 cells (Fig. S7A), and this effect could be blocked by wild-type HSD17B4 or K669 mutants re-expression (Fig. 7C, left

panel). Notably, E1 treatment distinctively inhibited the migration of MCF7 cells expressing wild-type HSD17B4 in a dramatical level (Fig. 7C, right panel). Next, we performed migration assays in 24-well chambers and found that HSD17B4 knockdown significantly decreased the number of migrating cells (Fig. S7B). Re-expression of either wild-type HSD17B4, as well as the K669R or K669Q mutant



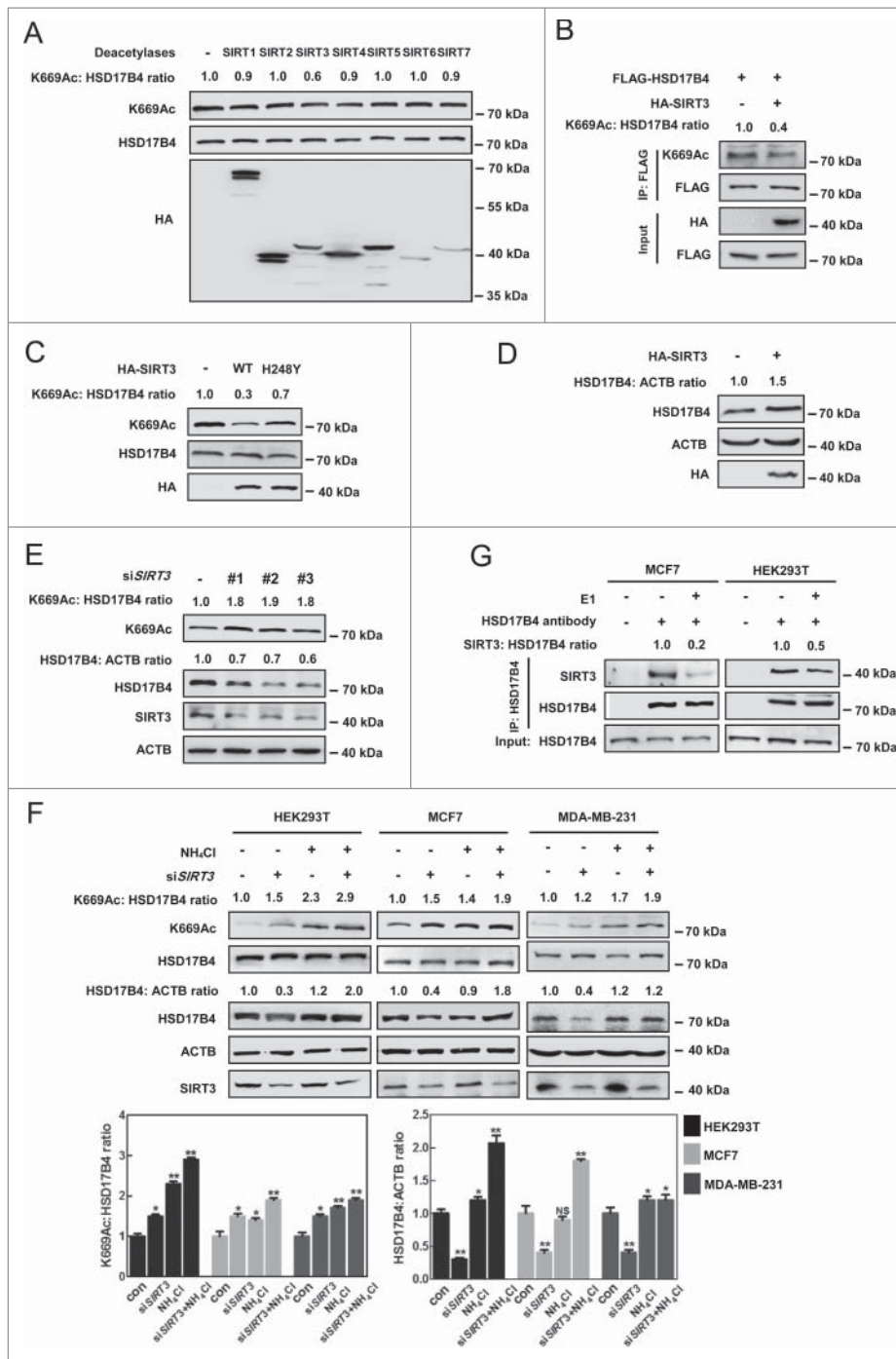


**Figure 6.** SIRT3 deacetylates HSD17B4 at K669. (A) Overexpression of SIRT3 exclusively decreases K669 acetylation level of endogenous HSD17B4. HEK293T cells were transfected with HA-tagged SIRT1-SIRT7 respectively. Cells lysates were analyzed using western blotting. (B) Overexpression of SIRT3 decreases the K669 acetylation level of wild-type HSD17B4. HA-tagged SIRT3 was cotransfected with FLAG-tagged HSD17B4 into HEK293T cells and the acetylation levels of HSD17B4 were determined by western blotting. (C) Wild-type SIRT3 but not the H248Y mutant decreases K669 acetylation of endogenous HSD17B4. HEK293T cells were transfected with wild-type HA-SIRT3 or the H248Y mutant. HSD17B4 K669 acetylation was detected using K669Ac antibody. (D) Overexpression of SIRT3 causes accumulation of HSD17B4 protein. HEK293T cells were transfected with HA-SIRT3 and protein levels of endogenous HSD17B4 were determined by western blotting. (E) SIRT3 knockdown increases HSD17B4 acetylation level at K669 while it decreases its protein levels. HEK293T cells were transfected with siSIRT3 or control. Cells were harvested 48 h after transfection, and cell lysates were analyzed by western blotting. (F) NH<sub>4</sub>Cl blocks HSD17B4 degradation induced by SIRT3 knockdown. HEK293T, MCF7 or MDA-MB-231 cells were transfected with siSIRT3 or control, followed by NH<sub>4</sub>Cl treatment for 24 h. Cells were harvested and cell lysates were determined by western blotting (upper panel). The relative HSD17B4 K669 acetylation compared with its total protein level and the relative HSD17B4 protein compared with the ACTB level were quantified (lower panel). \*denotes  $P < 0.05$ , \*\*denotes  $P < 0.01$ . Error bars represent  $\pm$  SD for triplicate experiments. (G) E1 decreases endogenous HSD17B4 binding with SIRT3. MCF7 or HEK293T cells were cultured with or without E1 for 24 h before harvest. The interaction between endogenous HSD17B4 and SIRT3 was determined by coIP and western blotting.

promoted cell migration (Fig. 7D and 7E). Consistently, the group expressing wild-type HSD17B4 showed a significant decrease of migrating cells compared with that of K669

mutants upon E1 treatment (Fig. 7D and 7E). Moreover, we performed an invasion assay in 24-well matrigel chambers, and obtained similar results that HSD17B4 knockdown



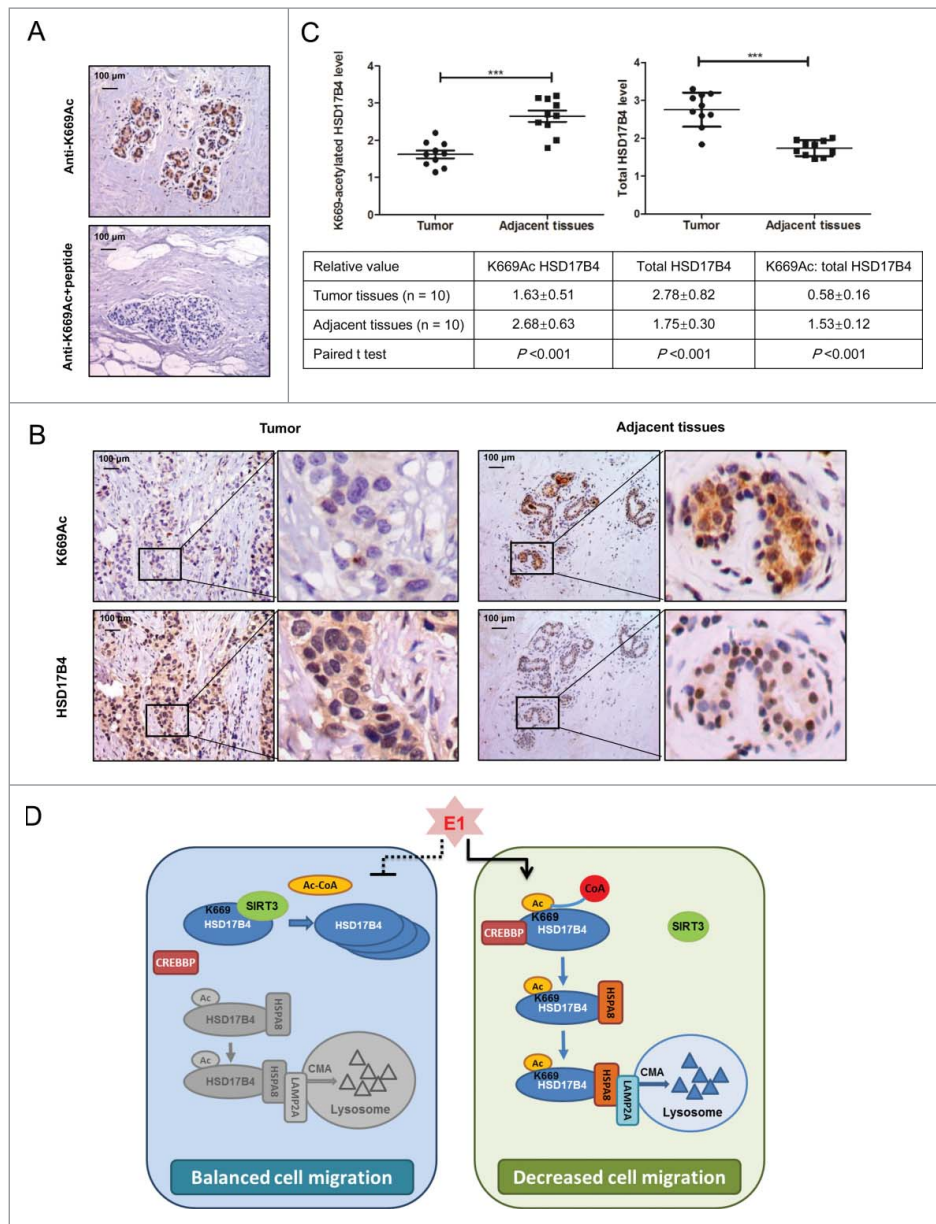


**Figure 8.** K669 acetylation of HSD17B4 is downregulated in human breast cancer samples. (A) Characterization of the anti-acetyl-HSD17B4 (K669) antibody for immunohistochemistry (IHC). Two images of a breast cancer were stained with the anti-acetyl-HSD17B4 (K669) antibody in the presence (lower panel) or absence (upper panel) of acetyl-K669 antigen peptide. Scale bars: 100  $\mu\text{m}$ . (B and C) Immunohistochemical staining of K669-acetylated and total HSD17B4 proteins in tumor and adjacent tissues. Examples are shown in (B) and the statistical analysis of all samples is shown in (C). Scale bars: 100  $\mu\text{m}$ . The intensities of the K669-acetylated (left panel) and total (right panel) HSD17B4 proteins were quantified, followed by statistical analysis. A total of 10 breast cancer tissues and 10 adjacent normal breast tissues were analyzed. The mean value of multiple samples and standard deviation are presented. (D) Working model. SIRT3 deacetylates HSD17B4 at K669 and stabilizes its protein level, while CREBBP acetylates HSD17B4 and promotes its lysosomal degradation via CMA. E1 increases the HSD17B4 acetylation level at K669 by enhancing HSD17B4 association with CREBBP, which leads to the degradation of HSD17B4, and therefore decreases the migration of breast cancer cells.

samples. To substantiate the finding that K669 acetylation promotes *HSD17B4* degradation, we explored the feasibility of determining the level of both total and K669-acetylated *HSD17B4* by immunohistochemistry in paraffin-embedded tissues. The anti-acetyl-*HSD17B4* (K669) antibody detected strong signals that were specifically blocked by the acetyl-K669 antigen peptide in paraffin-embedded tissues (Fig. 8A), indicating this antibody is suitable for immunohistochemistry. Taking advantage of this reagent, we then performed immunohistochemistry in the breast cancer samples and adjacent normal breast tissues. In most samples,

compared with the normal breast tissues, the levels of total *HSD17B4* were higher and the levels of relative K669-acetylated *HSD17B4* were lower in the tumor tissues (Fig. 8B and C). Statistical analyses of quantified images indicated that the differences between tumor and normal tissues in total *HSD17B4* protein levels ( $P < 0.001$ ), in K669-acetylated *HSD17B4* ( $P < 0.001$ ), and in the ratio of K669-acetylated *HSD17B4* versus total *HSD17B4* proteins ( $P < 0.001$ ) are all significant (Fig. 8C). These data further validate K669 acetylation of *HSD17B4* promotes its degradation in human breast cancer.

## Discussion

It is well known that acetylation is a broad posttranslational modification implicated in the regulation of various cellular processes.<sup>31,45,46</sup> There are more than 4000 potential nonnuclear acetylation substrates, and most of the acetylation substrates which have been found are intermediate metabolic enzymes. Acetylation modification can directly affect the function of enzymes via changing their activity, stability and other properties, and therefore modulated cellular metabolism.<sup>31,34,46,47</sup> In this study, we found that *HSD17B4* is regulated by acetylation, which promotes *HSD17B4* degradation. Acetylation modification of metabolic enzymes is very dynamic in response to different physiological signals, such as alteration of glucose, amino acids and other metabolites.<sup>33,34,47,48</sup> The present study demonstrates that E1 promotes *HSD17B4* acetylation via promoting the interaction between CREBBP and *HSD17B4* and decreases its stability as well. CREBBP and SIRT3 control the K669 acetylation level of *HSD17B4* in response to E1, and subsequently regulate its degradation (Fig. 8D).

Autophagy is a highly conserved process that allows cells, tissues and organs to survive onslaughts such as nutrient deprivation, inflammation, hypoxia and other stresses.<sup>49,50</sup> It is reported that acetylation, phosphorylation and ubiquitylation are crucial for autophagy induction, regulation and fine-tuning.<sup>33,34,51</sup> We presently indicate that *HSD17B4* acetylation at K669 stimulates its degradation via CMA, a selective degradation for proteins, especially those with a long-half-life.<sup>36</sup> A key step in CMA regulation is the interaction between chaperone HSPA8 and target proteins.<sup>52</sup> The acetylated *HSD17B4* displays a stronger interaction with HSPA8. For example, treatment with deacetylase inhibitors NAM or estrone, significantly increases the interaction between HSPA8 and *HSD17B4*. Furthermore, acetylated *HSD17B4* displays an enhanced interaction with lysosomes. Moreover, we found increased CMA activity and enhanced colocalization of *HSD17B4* and LAMP2A in E1-treated cells. Although the precise mechanism of acetylation in promoting the interaction between *HSD17B4* and HSPA8 is unclear, we speculate that acetylation of K669 may cause conformational changes in *HSD17B4*, thus the acetylated *HSD17B4* becomes accessible for recognition by HSPA8. Our study provides another example that acetylation regulates CMA by promoting the interaction between chaperone and target proteins.

Dysregulation of cellular metabolism is a hallmark of cancer.<sup>53</sup> *HSD17B4* has been implicated in the development of various cancers as previously mentioned.<sup>21-23</sup> In this study, we report that acetylation plays an important role in posttranslational regulation of *HSD17B4* and then affects breast cancer migration (Fig. 8D). *HSD17B4* is a multiple-function enzyme, involved in various processes of cellular metabolism.<sup>16,19,20</sup> With the exception of the inactivation of E2 to E1, *HSD17B4* participates in androgen metabolism, and in turn regulates multiple genes including genes involved in fatty acid and cholesterol metabolism.<sup>54</sup> Hypercholesterolemia, resulting from dysregulation of lipid metabolism, has been identified as an independent risk factor for breast cancer in postmenopausal women.<sup>55,56</sup> *HSD17B4* also metabolizes branched chain fatty acids in peroxisomes, which generates hydrogen peroxide, a potential source of

carcinogenic oxidative damage.<sup>57</sup> It was reported that as the D-bifunctional protein involved in peroxisomal branched chain acyl-CoAs  $\beta$ -oxidation pathway, *HSD17B4* is upregulated in prostate cancer at both mRNA and protein levels, accompanied by increased enzymatic activity, indicating that a promoting role of *HSD17B4* in oncogenes is through changing the cellular metabolism of cancer.<sup>58</sup> Moreover, 27-hydroxycholesterol, an abundant primary metabolite of cholesterol, induced EMT of MCF7 cells and increased ER-dependent growth and NR1H/LXR-dependent metastasis in mouse models of breast cancer.<sup>59</sup> *HSD17B4*, participating in cholesterol and bile acid metabolism, contributes to the balance of cholesterol and its metabolites.<sup>60</sup> Therefore *HSD17B4* might control EMT process in breast cancer by regulating 27-hydroxycholesterol metabolism.

In this study, we found that K669 acetylation reduces *HSD17B4* protein stability by promoting its CMA, which eliminates invasive and migratory properties of MCF7 cells, further contributing to a novel role of *HSD17B4* in malignant progression of breast cancer. The implication of this finding will present a potential prognostic marker of breast cancer and a candidate for therapeutics.

## Methods

### Cell culture and treatment

Cells were cultured in DMEM/High Glucose medium (HyClone, SH30234.01) supplemented with 10% fetal bovine serum (FBS; Biological Industries, 04-001-1ACS), 1% penicillin and streptomycin (HyClone, SV30010) at 37 °C, in a humidified atmosphere containing 5% CO<sub>2</sub>. For E1-added treatment, cells were first cultured in the medium which contained fetal bovine serum without hormone purchased from Biological Industries (04-201-1), then E1 (Sigma-Aldrich, 46573) of different concentrations was added into the medium to culture cells. Deacetylase-inhibitor treatments were performed by adding TSA (Cell Signaling Technology, 9950s; 10  $\mu$ M) and NAM (Cell Signaling Technology, N0636; 5 mM) to the culture medium 18 and 6 h before harvesting, respectively; both concentrations are final concentrations in the culture medium. Proteasomal/lysosomal inhibitor treatments were performed by adding chloroquine (Sigma-Aldrich, C6628; 100  $\mu$ M) for 8 h, MG132 (Abmole BioScience, M1902; 10  $\mu$ M) for 6 h, leupeptin (Selleckchem, S7380; 0.4 mM) for 24 h, NH<sub>4</sub>Cl (Sigma-Aldrich, A9434; 15 mM) for 24 h, wortmannin (Selleckchem, S2758; 100 nM) for 24 h, BAF (Selleckchem, S1413; 100 nM) for 8 h, respectively; all concentrations are final concentrations in the culture medium.

### Immunoprecipitation and western blotting

HEK293T, MCF7 or MDA-MB-231 cells were lysed in 0.2 to 0.3% Nonidet P40 (Sigma-Aldrich, 74388) buffer containing 150 mM NaCl, 50 mM Tris-HCl, pH 7.5 and multiple protease inhibitors (PMSF [Ameresco, 0754; 1 mM], aprotinin [Selleckchem, S7377; 1  $\mu$ g/ml], leupeptin [Selleckchem, S7380; 1  $\mu$ g/ml], pepstatin [Sigma-Aldrich, T6522; 1  $\mu$ g/ml], Na<sub>3</sub>VO<sub>4</sub> [Sigma-Aldrich, S6508; 1 mM], NaF [Sigma-Aldrich, S7920; 1 mM], TSA [1.5 mM], and NAM [15 mM], in final

concentrations). Cell lysates were incubated for 3 h at 4°C with anti-FLAG M2 agarose (Sigma-Aldrich, A2220) after removal of debris by centrifuging at 4°C, 16,200 g for 12 to 15 min. The beads, which contained immunoprecipitates, were washed 3 times with lysis buffer and centrifuged at 400 g for 1 min between each wash. Then beads were boiled and centrifuged at 4 °C before loading on 10% SDS-PAGE gels and transferred onto nitrocellulose membrane (GE Healthcare, 10402495) for western blotting analysis. The primary antibodies to FLAG (Sigma-Aldrich, F3165; 1:10,000 working dilution), HA (Santa Cruz Biotechnology, 7392; 1:1,000 working dilution), ACTB/ $\beta$ -actin (Sigma-Aldrich, A5441; 1:10,000 working dilution), LAMP2A (Abcam, 18528; 1:1,000 working dilution), HSPA8/HSC70 (Abcam, 19136; 1:1,000 working dilution), *HSD17B4* (Abcam, 128565; 1:1,000 working dilution), CREBBP (Abcam, 2832; 1:1,000 working dilution), SIRT3 (Abcam, 45067; 1:1,000 working dilution), acetylated-lysine (Cell Signaling Technology, 9441; 1:1,000 working dilution), and EMT marker (Cell Signaling Technology, 9782; 1:1,000 working dilution) were commercially obtained. The antibody specific to *HSD17B4* K669Ac was prepared commercially from immunized rabbits at Shanghai Genomic Inc. (1:500 working dilution).

#### Lysosome isolation and substrate protein uptake assay

Lysosomes were isolated by the following a previously described procedure.<sup>37</sup> Both lysosome binding and uptake assays were performed as described previously.<sup>61</sup>

#### Immunofluorescence staining

MCF7 cells were treated with E1 for 24 h. Thereafter cells were then fixed in 4% paraformaldehyde (Wuhan Goodbio technology, G1101), permeabilized with 0.2% Triton X-100 (Sigma-Aldrich, T8787), blocked by 5% bovine serum albumin (Amresco, 0332) in phosphate-buffered saline (Sigma-Aldrich, P5368), and then incubated with the indicated primary antibodies: LAMP2A (1:500 working dilution), HSPA8/HSC70 (1:500 working dilution), *HSD17B4* (1:500 working dilution), SIRT3 (1:500 working dilution), K669Ac (1:1000 working dilution). Detection was performed with corresponding fluorescent-conjugated secondary antibodies. Confocal fluorescence images were obtained with a confocal microscope (Fudan University, Shanghai; Leica TCS SP5, Germany). Relative colocalization was calculated with ImageJ software. Mean values were calculated from the individual distributions in 10 cells per condition.

#### siRNA transfection and RNA interference

Downregulation of *CREBBP* and *SIRT3* was performed by RNA interference. Synthetic *siRNA* oligo nucleotides were obtained commercially from Shanghai Genepharma Co, Ltd. List of effective sequences is as follows:

siCREBBP-1: 5'-GCAGCTGGTTCTACTGCTTdTdT-3'  
 siCREBBP-2: 5'-CCATTTCTCCTTCCCGAATdTdT-3'  
 siCREBBP-3: 5'-GGAAGCAGCTGTGTACCATdTdT-3'  
 siSIRT3-1: 5'-CCAGCAUGAAAUACAUUUAdTdT-3'  
 siSIRT3-2: 5'-CCAGUGGCAUUCAGACUUdTdT-3'  
 siSIRT3-3: 5'-GCCCGACAUGUGUUCUUdTdT-3'

All *siRNAs* were transfected with Lipofectamine 2000 (Invitrogen, 11668027) as per the manufacturer's protocol. The knockdown efficiency was verified by western blotting.

#### Knocking down and putting back stable cell lines

pMKO-sh*HSD17B4* and pMKO-sh*VEC* were constructed as short hairpin RNA vector. shRNA constructs including sh*HSD17B4* employed 3 effective sequences targeting the 3'-untranslated region as follows: 5'-AGGGCACACTACACTAT-TAAT-3'; 5'-GCCCAAGTCCTGTTTCCTTAG-3'; 5'-GCTC-TGCTTGTTCGTGTGTGT-3'. pMKO-sh*HSD17B4* or pMKO-sh*VEC* were cotransfected with vectors expressing gag and vsvg genes into HEK293T cells. Retroviral supernatants were harvested and applied to MCF7 cells. The *HSD17B4* knockdown cell pool was selected with puromycin (Amresco, J593; 5  $\mu$ g/ml final concentration) for 2 weeks. FLAG-tagged human wild-type, and the K669R and K669Q mutants of *HSD17B4* were cloned into the retroviral vector (pQCXIH; Clontech, 631516), after retroviral production, sh*HSD17B4* stable cells were infected with the prepared virus for 48 h and screened using hygromycin (Amresco, K547; 350  $\mu$ g/ml final concentration) for at least 2 wk. All vectors and stable cell lines were deposited in Cancer Metabolism Laboratory of Fudan University.

#### Cell migration and wound healing assays

MCF-7 cells ( $2 \times 10^5$ ) stably expressing WT *HSD17B4*, *HSD17B4*<sup>K669R</sup> and *HSD17B4*<sup>K669Q</sup> were suspended with 100  $\mu$ L serum-free medium, loaded in each insert of a transwell chamber (Corning, 3422) and treated with E1. Medium containing 10% FBS was placed in the wells below the insert. After incubation for 48 h, cells that migrated through the membrane were fixed in methanol and stained with crystal violet. The number of migrated cells was counted. The photographs were taken from 5 randomly visions by a microscopy. Quantitative analysis of the cell migration was performed using ImageJ. 3 separate experiments were performed. For the wound-healing assay, monolayer cells were wounded with a sterile plastic tip. Cell migration was observed by microscopy 24 h later.

#### Cell invasion assay

MCF-7 cells ( $2 \times 10^5$ ) stably expressing *HSD17B4*<sup>WT</sup>, *HSD17B4*<sup>K669R</sup> or *HSD17B4*<sup>K669Q</sup> were suspended with 100  $\mu$ L serum-free medium, then placed into the upper matrigel transwell chamber (Corning Biocoat, 354480) in serum-free medium. Medium containing 10% FBS was placed in the chamber below the insert. Subsequent to 48 h of incubation at 37 °C, the invasive cells attached to the lower membrane of the inserts were fixed in methanol and stained with crystal violet, then counted using microscopy. Quantitative analysis of the cell invasion was performed using ImageJ. 3 separate experiments were performed.

#### Breast tumor samples and immunohistochemistry

Breast tumor samples were acquired from the Shanghai Huashan hospital of Fudan University. A physician obtained

informed consent from the patients. The procedures related to human subjects were approved by Ethic Committee of the school of Basic Medical Sciences, Fudan University. Immunohistochemistry (IHC) was performed as previously described.<sup>62</sup> To quantify the IHC result of positive staining, 5 random areas in each tissue sample were microscopically examined and analyzed by an experienced pathologist. The average of staining score was calculated by dividing the positive areas with total areas. Data obtained were expressed as mean values  $\pm$  SD.

### Statistical analysis

Two-tailed Student *t* tests were used for all comparisons, including qPCR analysis. All values included in the figures represent mean  $\pm$  SD. Error bars represent  $\pm$  SD for triplicate experiments. The statistical significance is indicated as asterisks (\*). The 2-sided *P* value of  $< 0.05$  was considered to be statistically significant (\**P*  $< 0.05$ , \*\**P*  $< 0.01$ , \*\*\**P*  $< 0.001$ ).

### Abbreviations

3-MA	3-methyladenine
BAF	bafilomycin A <sub>1</sub>
CDH1	E-Cadherin/cadherin 1
CDH2	N-Cadherin/cadherin 2
CLQ	chloroquine
CMA	chaperone-mediated autophagy
CREBBP/CBP	CREB binding protein
E1	estrone
E2	estradiol
EMT	epithelial-mesenchymal transition
EP300	E1A binding protein p300
HCC	human hepatocellular carcinoma
HSD17Bs	17 $\beta$ -hydroxysteroid dehydrogenases
HSD17B4/DBP/MFE-2/MFP-2	hydroxysteroid 17- $\beta$ dehydrogenase 4
IHC	immunohistochemistry
KAT2A/GCN5	lysine acetyltransferase 2A
KAT2B/PCAF	lysine acetyltransferase 2B
NAM	nicotinamide
TSA	trichostatin A
VIM	vimentin

### Disclosure of potential conflicts of interest

No potential conflicts of interest were disclosed.

### Acknowledgments

We thank the members of the Fudan Cancer Metabolism Laboratory for discussion throughout this study. We also thank the Biomedical Core Facility of Fudan University for their technical support.

### Funding

This work was supported by MOST (2015CB910401), NSFC (Grant No.81430057, 81572686, 81225016, 31271454).

### References

- [1] Siegel R, Naishadham D, Jemal A. Cancer statistics, 2013. *CA Cancer J Clin* 2013; 63:11-30; <http://dx.doi.org/10.3322/caac.21166>
- [2] Chetrite G, Kloosterboer HJ, Pasqualini JR. Effect of tibolone (Org OD14) and its metabolites on estrone sulphatase activity in MCF-7 and T-47D mammary cancer cells. *Anticancer Res* 1997; 17:135-40; PMID:9066643
- [3] Henderson BE, Ross RK, Pike MC, Casagrande JT. Endogenous hormones as a major factor in human cancer. 1982
- [4] Yager JD, Davidson NE. Estrogen carcinogenesis in breast cancer. *N Engl J Med* 2006; 354:270-82; PMID:16421368; <http://dx.doi.org/10.1056/NEJMra050776>
- [5] Platet N, Cathiard AM, Gleizes M, Garcia M. Estrogens and their receptors in breast cancer progression: a dual role in cancer proliferation and invasion. *Crit Rev Oncol Hematol* 2004; 51:55-67; PMID:15207254; <http://dx.doi.org/10.1016/j.critrevonc.2004.02.001>
- [6] Maynadier M, Nirde P, Ramirez JM, Cathiard AM, Platet N, Chambon M, Garcia M. Role of estrogens and their receptors in adhesion and invasiveness of breast cancer cells. *Adv Exp Med Biol* 2008; 617:485-91; PMID:18497073; [http://dx.doi.org/10.1007/978-0-387-69080-3\\_48](http://dx.doi.org/10.1007/978-0-387-69080-3_48)
- [7] Samavat H, Kurzer MS. Estrogen metabolism and breast cancer. *Cancer Lett* 2015; 356:231-43; PMID:24784887; <http://dx.doi.org/10.1016/j.canlet.2014.04.018>
- [8] Aka JA, Mazumdar M, Lin SX. Reductive 17beta-hydroxysteroid dehydrogenases in the sulfatase pathway: critical in the cell proliferation of breast cancer. *Mol Cell Endocrinol* 2009; 301:183-90; PMID:19038308; <http://dx.doi.org/10.1016/j.mce.2008.10.042>
- [9] Ayan D, Maltais R, Roy J, Poirier D. A new nonestrogenic steroidal inhibitor of 17beta-hydroxysteroid dehydrogenase type I blocks the estrogen-dependent breast cancer tumor growth induced by estrone. *Mol Cancer Ther* 2012; 11:2096-104; PMID:22914440; <http://dx.doi.org/10.1158/1535-7163.MCT-12-0299>
- [10] Lin SX, Yang F, Jin JZ, Breton R, Zhu DW, Luu-The V, Labrie F. Subunit identity of the dimeric 17 beta-hydroxysteroid dehydrogenase from human placenta. *J BIOL CHEM* 1992; 267:16182-7; PMID:1322895
- [11] Gunnarsson C, Olsson BM, Stal O. Abnormal expression of 17beta-hydroxysteroid dehydrogenases in breast cancer predicts late recurrence. *Cancer Res* 2001; 61:8448-51; PMID:11731426
- [12] Oduwole OO, Li Y, Isomaa VV, Mantyniemi A, Pulkka AE, Soini Y, Vihko PT. 17beta-hydroxysteroid dehydrogenase type 1 is an independent prognostic marker in breast cancer. *Cancer Res* 2004; 64:7604-9; PMID:15492288; <http://dx.doi.org/10.1158/0008-5472.CAN-04-0446>
- [13] Nguyen BL, Chetrite G, Pasqualini JR. Transformation of estrone and estradiol in hormone-dependent and hormone-independent human breast cancer cells. Effects of the antiestrogen ICI 164,384, danazol, and promegestone (R-5020). *Breast Cancer Res Treat* 1995; 34:139-46; <http://dx.doi.org/10.1007/BF00665786>
- [14] Jansson A, Delander L, Gunnarsson C, Fornander T, Skoog L, Nordenskjoeld B, Stal O. Ratio of 17HSD1 to 17HSD2 protein expression predicts the outcome of tamoxifen treatment in postmenopausal breast cancer patients. *Clin Cancer Res* 2009; 15:3610-6; PMID:19401349; <http://dx.doi.org/10.1158/1078-0432.CCR-08-2599>
- [15] Zhang CY, Wang WQ, Chen J, Lin SX. Reductive 17beta-hydroxysteroid dehydrogenases which synthesize estradiol and inactivate dihydrotestosterone constitute major and concerted players in ER+ breast cancer cells. *J Steroid Biochem Mol Biol* 2015; 150:24-34; PMID:25257817; <http://dx.doi.org/10.1016/j.jsbmb.2014.09.017>
- [16] Breitling R, Marijanovic Z, Perovic D, Adamski J. Evolution of 17beta-HSD type 4, a multifunctional protein of beta-oxidation. *Mol Cell Endocrinol* 2001; 171:205-10; PMID:11165031; [http://dx.doi.org/10.1016/S0303-7207\(00\)00415-9](http://dx.doi.org/10.1016/S0303-7207(00)00415-9)
- [17] Moller G, Leenders F, van Grunsven EG, Dolez V, Qualmann B, Kesels MM, Markus M, Krazeisen A, Husen B, Wanders RJ, de Launoit Y, Adamski J. Characterization of the *HSD17B4* gene: D-specific multifunctional protein 2/17beta-hydroxysteroid dehydrogenase IV.

- J Steroid Biochem Mol Biol 1999; 69:441-6; PMID:10419023; [http://dx.doi.org/10.1016/S0960-0760\(99\)00066-7](http://dx.doi.org/10.1016/S0960-0760(99)00066-7)
- [18] Deluca D, Moller G, Rosinus A, Elger W, Hillisch A, Adamski J. Inhibitory effects of fluorine-substituted estrogens on the activity of 17beta-hydroxysteroid dehydrogenases. *Mol Cell Endocrinol* 2006; 248:218-24; PMID:16406285; <http://dx.doi.org/10.1016/j.mce.2005.11.037>
- [19] Peltoketo H, Vihko P, Vihko R. Regulation of estrogen action: role of 17 beta-hydroxysteroid dehydrogenases. *Vitam Horm* 1999; 55:353-98; PMID:9949685; [http://dx.doi.org/10.1016/S0083-6729\(08\)60939-5](http://dx.doi.org/10.1016/S0083-6729(08)60939-5)
- [20] Baes M, Huyghe S, Carmeliet P, Declercq PE, Collen D, Mannaerts GP, Van Veldhoven PP. Inactivation of the peroxisomal multifunctional protein-2 in mice impedes the degradation of not only 2-methyl-branched fatty acids and bile acid intermediates but also of very long chain fatty acids. *J BIOL CHEM* 2000; 275:16329-36; PMID:10748062; <http://dx.doi.org/10.1074/jbc.M001994200>
- [21] Rasiyah KK, Gardiner-Garden M, Padilla EJ, Moller G, Kench JG, Alles MC, Eggleton SA, Stricker PD, Adamski J, Sutherland RL, Henshall SM, Hayes VM. *HSD17B4* overexpression, an independent biomarker of poor patient outcome in prostate cancer. *Mol Cell Endocrinol* 2009; 301:89-96; PMID:19100308; <http://dx.doi.org/10.1016/j.mce.2008.11.021>
- [22] Lu X, Ma P, Shi Y, Yao M, Hou L, Zhang P, Jiang L. NF-kappaB increased expression of 17beta-hydroxysteroid dehydrogenase 4 promotes HepG2 proliferation via inactivating estradiol. *MOL Cell Endocrinol* 2015; 401:1-11; PMID:25448063; <http://dx.doi.org/10.1016/j.mce.2014.11.016>
- [23] English MA, Kane KF, Cruickshank N, Langman MJ, Stewart PM, Hewison M. Loss of estrogen inactivation in colonic cancer. *J Clin Endocrinol Metab* 1999; 84:2080-5; PMID:10372714; <http://dx.doi.org/10.1210/jcem.84.6.5772>
- [24] McMichael AJ, Potter JD. Colon cancer and sex. 1982
- [25] Nagayoshi Y, Ohba T, Yamamoto H, Miyahara Y, Tashiro H, Katabuchi H, Okamura H. Characterization of 17beta-hydroxysteroid dehydrogenase type 4 in human ovarian surface epithelial cells. *Mol Hum Reprod* 2005; 11:615-21; PMID:16219629; <http://dx.doi.org/10.1093/molehr/gah215>
- [26] Maleki J, Nourbakhsh M, Shabani M, Korani M, Nourazarian SM, Ostadali DM, Moghadasi MH. 17beta-Estradiol Stimulates Generation of Reactive Species Oxygen and Nitric Oxide in Ovarian Adenocarcinoma Cells (OVCAR 3). 2015
- [27] Liu P, Kimmoun E, Legrand A, Sauvanet A, Degott C, Lardeux B, Bernuau D. Activation of NF-kappa B, AP-1 and STAT transcription factors is a frequent and early event in human hepatocellular carcinomas. *J Hepatol* 2002; 37:63-71; PMID:12076863; [http://dx.doi.org/10.1016/S0168-8278\(02\)00064-8](http://dx.doi.org/10.1016/S0168-8278(02)00064-8)
- [28] Flanagan JM, Munoz-Alegre M, Henderson S, Tang T, Sun P, Johnson N, Fletcher O, Dos SSI, Peto J, Boshoff C, Narod S, Petronis A. Gene-body hypermethylation of ATM in peripheral blood DNA of bilateral breast cancer patients. *Hum Mol Genet* 2009; 18:1332-42; PMID:19153073; <http://dx.doi.org/10.1093/hmg/ddp033>
- [29] Fiegl H, Millinger S, Goebel G, Muller-Holzner E, Marth C, Laird PW, Widschwendter M. Breast cancer DNA methylation profiles in cancer cells and tumor stroma: association with HER-2/neu status in primary breast cancer. *Cancer Res* 2006; 66:29-33; PMID:16397211; <http://dx.doi.org/10.1158/0008-5472.CAN-05-2508>
- [30] Muller HM, Widschwendter A, Fiegl H, Ivarsson L, Goebel G, Perkmann E, Marth C, Widschwendter M. DNA methylation in serum of breast cancer patients: an independent prognostic marker. *Cancer Res* 2003; 63:7641-5; PMID:14633683
- [31] Choudhary C, Kumar C, Gnani F, Nielsen ML, Rehman M, Walther TC, Olsen JV, Mann M. Lysine acetylation targets protein complexes and co-regulates major cellular functions. *Science* 2009; 325:834-40; PMID:19608861; <http://dx.doi.org/10.1126/science.1175371>
- [32] Lundby A, Lage K, Weinert BT, Bekker-Jensen DB, Secher A, Skovgaard T, Kelstrup CD, Dmytryiev A, Choudhary C, Lundby C, Olsen JV. Proteomic analysis of lysine acetylation sites in rat tissues reveals organ specificity and subcellular patterns. *Cell Rep* 2012; 2:419-31; PMID:22902405; <http://dx.doi.org/10.1016/j.celrep.2012.07.006>
- [33] Lv L, Li D, Zhao D, Lin R, Chu Y, Zhang H, Zha Z, Liu Y, Li Z, Xu Y, Wang G, Huang Y, Xiong Y, Guan KL, Lei QY. Acetylation targets the M2 isoform of pyruvate kinase for degradation through chaperone-mediated autophagy and promotes tumor growth. *Mol Cell* 2011; 42:719-30; PMID:21700219; <http://dx.doi.org/10.1016/j.molcel.2011.04.025>
- [34] Zhao D, Zou SW, Liu Y, Zhou X, Mo Y, Wang P, Xu YH, Dong B, Xiong Y, Lei QY, Guan KL. Lysine-5 acetylation negatively regulates lactate dehydrogenase A and is decreased in pancreatic cancer. *Cancer Cell* 2013; 23:464-76; PMID:23523103; <http://dx.doi.org/10.1016/j.ccr.2013.02.005>
- [35] Jiang W, Wang S, Xiao M, Lin Y, Zhou L, Lei Q, Xiong Y, Guan KL, Zhao S. Acetylation regulates gluconeogenesis by promoting PEPCK1 degradation via recruiting the UBR5 ubiquitin ligase. *Mol Cell* 2011; 43:33-44; PMID:21726808; <http://dx.doi.org/10.1016/j.molcel.2011.04.028>
- [36] Mizushima N, Levine B, Cuervo AM, Klionsky DJ. Autophagy fights disease through cellular self-digestion. *Nature* 2008; 451:1069-75; PMID:18305538; <http://dx.doi.org/10.1038/nature06639>
- [37] Cuervo AM, Knecht E, Terlecky SR, Dice JF. Activation of a selective pathway of lysosomal proteolysis in rat liver by prolonged starvation. *Am J Physiol* 1995; 269:C1200-8; PMID:7491910
- [38] Wing SS, Chiang HL, Goldberg AL, Dice JF. Proteins containing peptide sequences related to Lys-Phe-Glu-Arg-Gln are selectively depleted in liver and heart, but not skeletal muscle, of fasted rats. *Biochem J* 1991; 275(Pt 1):165-9; PMID:2018472; <http://dx.doi.org/10.1042/bj2750165>
- [39] Agarraberes FA, Terlecky SR, Dice JF. An intralysosomal hsp70 is required for a selective pathway of lysosomal protein degradation. *J Cell Biol* 1997; 137:825-34; PMID:9151685; <http://dx.doi.org/10.1083/jcb.137.4.825>
- [40] Cuervo AM, Dice JF. Unique properties of lamp2a compared to other lamp2 isoforms. *J Cell Sci* 2000; 113(Pt 24):4441-50; PMID:11082038
- [41] Patel B, Cuervo AM. Methods to study chaperone-mediated autophagy. *Methods* 2015; 75:133-40; PMID:25595300; <http://dx.doi.org/10.1016/j.ymeth.2015.01.003>
- [42] Kaushik S, Cuervo AM. Methods to monitor chaperone-mediated autophagy. *Methods Enzymol* 2009; 452:297-324; PMID:19200890; [http://dx.doi.org/10.1016/S0076-6879\(08\)03619-7](http://dx.doi.org/10.1016/S0076-6879(08)03619-7)
- [43] Nieto MA, Cano A. The epithelial-mesenchymal transition under control: global programs to regulate epithelial plasticity. *Semin Cancer Biol* 2012; 22:361-8; PMID:22613485; <http://dx.doi.org/10.1016/j.semcancer.2012.05.003>
- [44] Gupta GP, Massague J. Cancer metastasis: building a framework. *CELL* 2006; 127:679-95; PMID:17110329; <http://dx.doi.org/10.1016/j.cell.2006.11.001>
- [45] Kim SC, Sprung R, Chen Y, Xu Y, Ball H, Pei J, Cheng T, Kho Y, Xiao H, Xiao L, Grishin NV, White M, Yang XJ, Zhao Y. Substrate and functional diversity of lysine acetylation revealed by a proteomics survey. *Mol Cell* 2006; 23:607-18; PMID:16916647; <http://dx.doi.org/10.1016/j.molcel.2006.06.026>
- [46] Zhao S, Xu W, Jiang W, Yu W, Lin Y, Zhang T, Yao J, Zhou L, Zeng Y, Li H, Li Y, Shi J, An W, Hancock SM, He F, Qin L, Chin J, Yang P, Chen X, Lei Q, Xiong Y, Guan KL. Regulation of cellular metabolism by protein lysine acetylation. *SCIENCE* 2010; 327:1000-4; PMID:20167786; <http://dx.doi.org/10.1126/science.1179689>
- [47] Li T, Liu M, Feng X, Wang Z, Das I, Xu Y, Zhou X, Sun Y, Guan KL, Xiong Y, Lei QY. Glyceroldehyde-3-phosphate dehydrogenase is activated by lysine 254 acetylation in response to glucose signal. *J Biol Chem* 2014; 289:3775-85; PMID:24362262; <http://dx.doi.org/10.1074/jbc.M113.531640>
- [48] Yang HB, Xu YY, Zhao XN, Zou SW, Zhang Y, Zhang M, Li JT, Ren F, Wang LY, Lei QY. Acetylation of MAT I1alpha represses tumour cell growth and is decreased in human hepatocellular cancer. *Nat Commun* 2015; 6:6973; PMID:25925782; <http://dx.doi.org/10.1038/ncomms7973>
- [49] Saha T. LAMP2A overexpression in breast tumors promotes cancer cell survival via chaperone-mediated autophagy. *Autophagy* 2012; 8:1643-56; PMID:22874552; <http://dx.doi.org/10.4161/auto.21654>

- [50] Xie W, Zhang L, Jiao H, Guan L, Zha J, Li X, Wu M, Wang Z, Han J, You H. Chaperone-mediated autophagy prevents apoptosis by degrading BBC3/PUMA. *Autophagy* 2015; 11:1623-35; PMID:26212789; <http://dx.doi.org/10.1080/15548627.2015.1075688>
- [51] McEwan DG, Dikic I. The Three Musketeers of Autophagy: phosphorylation, ubiquitylation and acetylation. *Trends Cell Biol* 2011; 21:195-201; PMID:21277210; <http://dx.doi.org/10.1016/j.tcb.2010.12.006>
- [52] Stricher F, Macri C, Ruff M, Muller S. HSPA8/HSC70 chaperone protein: structure, function, and chemical targeting. *Autophagy* 2013; 9:1937-54; PMID:24121476; <http://dx.doi.org/10.4161/auto.26448>
- [53] Hanahan D, Weinberg RA. Hallmarks of Cancer: The Next Generation. *Cell* 2011; 144:646-74; PMID:21376230; <http://dx.doi.org/10.1016/j.cell.2011.02.013>
- [54] Swinnen JV, Ulrix W, Heyns W, Verhoeven G. Coordinate regulation of lipogenic gene expression by androgens: evidence for a cascade mechanism involving sterol regulatory element binding proteins. *Proc Natl Acad Sci U S A* 1997; 94:12975-80; PMID:9371785; <http://dx.doi.org/10.1073/pnas.94.24.12975>
- [55] Boyd NF, McGuire V. Evidence of association between plasma high-density lipoprotein cholesterol and risk factors for breast cancer. *J Natl Cancer Inst* 1990; 82:460-8; PMID:2313717; <http://dx.doi.org/10.1093/jnci/82.6.460>
- [56] Kitahara CM, Berrington DGA, Freedman ND, Huxley R, Mok Y, Jee SH, Samet JM. Total cholesterol and cancer risk in a large prospective study in Korea. *J Clin Oncol* 2011; 29:1592-8; PMID:21422422; <http://dx.doi.org/10.1200/JCO.2010.31.5200>
- [57] Tamatani T, Turk P, Weitzman S, Oyasu R. Tumorigenic conversion of a rat urothelial cell line by human polymorphonuclear leukocytes activated by lipopolysaccharide. *Jpn J Cancer Res* 1999; 90:829-36; PMID:10543254; <http://dx.doi.org/10.1111/j.1349-7006.1999.tb00823.x>
- [58] Zha S, Ferdinandusse S, Hicks JL, Denis S, Dunn TA, Wanders RJ, Luo J, De Marzo AM, Isaacs WB. Peroxisomal branched chain fatty acid beta-oxidation pathway is upregulated in prostate cancer. *Prostate* 2005; 63:316-23; PMID:15599942; <http://dx.doi.org/10.1002/pros.20177>
- [59] Nelson ER, Wardell SE, Jasper JS, Park S, Suchindran S, Howe MK, Carver NJ, Pillai RV, Sullivan PM, Sondhi V, Umetani M, Geradts J, McDonnell DP. 27-Hydroxycholesterol links hypercholesterolemia and breast cancer pathophysiology. *Science* 2013; 342:1094-8; PMID:24288332; <http://dx.doi.org/10.1126/science.1241908>
- [60] Poirier Y, Antonenkov VD, Glumoff T, Hiltunen JK. Peroxisomal beta-oxidation—a metabolic pathway with multiple functions. *Biochim Biophys Acta* 2006; 1763:1413-26; PMID:17028011; <http://dx.doi.org/10.1016/j.bbamcr.2006.08.034>
- [61] Cuervo AM, Stefanis L, Fredenburg R, Lansbury PT, Sulzer D. Impaired degradation of mutant alpha-synuclein by chaperone-mediated autophagy. *Science* 2004; 305:1292-5; PMID:15333840; <http://dx.doi.org/10.1126/science.1101738>
- [62] Lei Q, Jiao J, Xin L, Chang CJ, Wang S, Gao J, Gleave ME, Witte ON, Liu X, Wu H. NKX3.1 stabilizes p53, inhibits AKT activation, and blocks prostate cancer initiation caused by PTEN loss. *Cancer Cell* 2006; 9:367-78; PMID:16697957; <http://dx.doi.org/10.1016/j.ccr.2006.03.031>